Available online at www.sciencedirect.com
SCIENCE DIRECT®
Analytical Biochemistry 330 (2004) 10–20
ANALYTICAL BIOCHEMISTRY
www.elsevier.com/locate/yabio

Environmentally low-temperature kinetic and thermodynamic study of lactate dehydrogenase from Atlantic cod (*G. morhua*) using a 96-well microplate technique

Maxim V. Zakhartsev,[a,*,1] Hans O. Pörtner,[b] and Ronny Blust[a]

[a] *Department of Biology, University of Antwerp–RUCA, Groenenborgerlaan 171, B-2020 Antwerp, Belgium*
[b] *Marine Biology/Ecological Physiology, Alfred Wegener Institute for Polar and Marine Research, D-27568 Bremerhaven, Germany*

Received 15 September 2003
Available online 6 May 2004

Abstract

Analyses of temperature-dependent kinetic parameters in enzymes extracted from tissues of ectothermic animals are usually carried out within the range of physiological temperatures (0–40 °C). However, multisample spectrophotometers (so-called microplate readers) with efficient wide-range temperature control (including cooling) have previously been unavailable. This limits the statistical quality of the measurements. A temperature-controlled microplate was designed for a 96-well microplate reader to overcome this limitation. This so-called T-microplate is able to control assay temperature between the freezing point of a liquid sample and 60 °C with high stability and accuracy in any data acquisition mode. At 4 °C the accuracy of the temperature control was ±0.1 °C and temperature homogeneity across the microplate was ±0.3 °C. As examples, analyses of the temperature dependence of Michaelis–Menten ($K_m^{\prime PYR}$) and substrate inhibition (K_{si}^{PYR}) constants for pyruvate, of the maximal rate of reaction (V'_{max}), of the apparent Arrhenius activation energy (E_A), and of the Gibbs free-energy change ($\Delta G^{\ddagger}$) of lactate dehydrogenases from muscle of Atlantic cod *Gadus morhua* acclimated to 4 °C are described. The large dataset obtained allowed evaluation of a new mechanism of metabolic compensation in response to seasonal temperature change.

Keywords: Arrhenius activation energy; Enzyme kinetics; Enzyme thermodynamics; Lactate dehydrogenase; Microplate reader; Temperature

Analysis of temperature-specific activities and kinetic parameters of enzymes extracted from ectothermic animals has to set assay temperatures to those naturally experienced by the animals, because the results obtained must support ecologically relevant interpretations. In the case of marine fishes from temperate latitudes temperatures usually range between 0 and 20 °C.

Traditional spectrophotometric analyses of the enzyme activities by use of a temperature-controlled water jacket around a single cuvette holder are well known. The external thermostat provides constant and accurate temperature control over a broad temperature range. However, the numbers of samples handled for simultaneous reading in such spectrophotometers are usually limited to between one and six. A traditional spectrophotometric cuvette has a relatively large inside volume (between 1 and 3 ml), which requires excess quantities of reagents. The restriction of the number of samples may also affect the statistical quality of the collected data due to systematic errors introduced by variable pipetting, which is associated with reduced repeatability and larger standard errors (±SE). Additionally, the total time spent during the analyses of extracts from a single fish results in limited data sets.

Measurements of the temperature dependence of enzyme kinetic parameters for large numbers of animals

* Corresponding author. Fax: +49-421-200-3229.
E-mail address: m.zakhartsev@iu-bremen.de (M.V. Zakhartsev).
[1] Present address: Biochemical Engineering, International University of Bremen, Campus Ring 1, D- 28759 Bremen, Germany.

0003-2697/$ - see front matter © 2004 Elsevier Inc. All rights reserved.
doi:10.1016/j.ab.2004.03.070

($n > 7$) using a single-sample spectrophotometer usually is difficult because of statistical requirements [1–3]. To avoid these restrictions it is better to use multisample spectrophotometers (so-called microplate readers). However, they have never been used for this purpose, because of their limited capacity to control temperature over a broad range (including cooling). This conclusion has emerged on the basis of analysis of scientific publications concerning research on the temperature dependence of enzymes from ectothermic animals and because microplate readers with cooling capacities were unavailable [4]. In most cases, the commercial microplate readers with temperature control have their lowest point of stable temperature control about 4–6 °C above room temperature, and the highest point is at about 40–50 °C [4]. Temperature regulation in the microplate chamber of such models is usually achieved through an electric heater, a fan, efficient insulation, and a temperature sensor (temperature feedback close-loop control algorithms) without forced cooling. Such a temperature control mechanism results in relatively high temperature inertia and relatively low temperature homogeneity/accuracy across the microplate even under mild conditions. For instance, the dual-scanning microplate spectrofluorometer SPECTRAmax GEMINI (Molecular Devices, USA) reaches a stable 37 °C in the microplate chamber within about 30 min starting from room temperature, and the uniformity of temperature control across the microplate is ±0.5 °C at 37 °C [5].

These restrictions in the width of temperature range, speed, accuracy, and homogeneity of temperature control were overcome by the recent improvement of temperature control in a microplate reader [6]. A new approach uses delivery of a heat-carrier with the desired temperature from an external thermostat directly inside the microplate. Such an approach allows precise, fast, and stable temperature control over a broad range. The present paper briefly describes a new device for temperature control in a 96-well microplate reader (T-microplate) that allows collection of statistically sufficient data quantities for relatively large numbers of animals ($n = 21$) within a relatively short time (10 days), which would not be possible to obtain using traditional techniques. The capacity of the T-microplate is exemplified by analyses of the temperature-dependent kinetic and thermodynamic parameters of lactate dehydrogenases (LDH)[2] in crude homogenates of white muscle of Atlantic cod *Gadus morhua* acclimated to 4 °C.

It is well documented that LDH from most ectothermic animals displays clear substrate inhibition kinetics (Fig. 1) [7–16], which is described by following mechanism [2]:

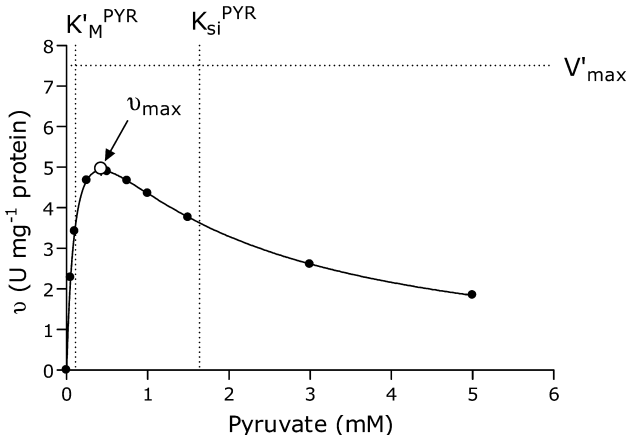

Fig. 1. Simulated kinetic curve for the LDH suite (LDH-iso-/allozyme mixture in crude homogenates) in muscle of Atlantic cod *Gadus morhua* acclimated to 4 °C. The simulation is based on averaged kinetic parameters obtained for this temperature from 21 individual fishes. The number of enzymatic reactions, which were read at 10 pyruvate concentrations in triplicate for all 21 fishes is $n = 630$ (Table 2). The assay temperature was 4 °C. The kinetic parameters (V'_{max}, K'^{PYR}_m, K^{PYR}_{si}) were calculated according to Eq. (2); the actual maximal rate of the reaction (υ_{max}; open circles) was calculated according to Eq. (4).

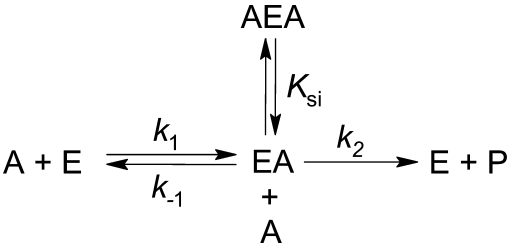

(1)

Materials and methods

Animals and tissue sampling

One-year-old Norwegian coastal cod *G. morhua* were acclimated at 4 °C in flow-through tanks during 408 days (University of Bergen, Norway); 4 °C is in the low range of temperatures that the fish normally experience in their natural environment during the winter season. During the acclimation experiment, the fish were fed in excess with commercial dry food. At the end of acclimation the fish were killed with 1 g L^{-1} 3-aminobenhoic acid (MS222) [17] and samples of white muscle were taken. Sampling time was reduced as much as possible; in general it took less than 3 min from the killing of the fish until sample fixation. The samples were freeze-clamped in liquid nitrogen (−195 °C), transported on dry ice (−60–70 °C), and stored in a deep frozen (−80 °C).

LDH extraction

Pieces of frozen white muscle were weighed and 1% tissue homogenates (w/v) were prepared (Ultra-Turrax

[2] *Abbreviation used:* LDH, lactate dehydrogenase.

T25) in ice-cold 50 mM Hepes, 100 mM KCl, pH 7.00 (at 20 °C), and then the homogenates were centrifuged at $15 \times 10^3 g$ for 20 min at 4 °C [18]. The supernatant was collected and used for subsequent kinetic and thermodynamic analyses. Hepes was chosen as a buffer that does not interfere with the NanoOrange total protein quantification method and that displays a temperature-dependent pH change by −0.015 pH °C^{-1} [19], which is essential for studying kinetics [20] and almost identical to the temperature-dependent change of intracellular pH in marine fish [21].

LDH kinetic studies at saturating cofactor levels in crude homogenates

To measure the initial rate of the reaction the enzyme concentration was adjusted such that the reaction rate was linear (first order) over 3 min. The decrease in optical density was less than 10% during this period. The reaction was monitored using a Bio-Rad 3550-UV microplate reader (96-well format) at 340 nm. Intensive shaking for 2 s preceded every reading of optical density (once every 15 s) during kinetic data acquisition.

The reaction was started by mixing 100 µl of diluted homogenate (enzyme concentration set according to assay temperature; Table 1) with 200 µl of assay medium, which was preequilibrated to assay temperature. The final 300 µl of assay medium always contained 200 µM β-NADH at saturation level for LDH of marine fish [9] pyruvate from 0 to 5 mM (0, 0.05, 0.1, 0.25, 0.5, 0.75, 1, 1.5, 3, and 5 mM) in 50 mM Hepes, pH 7.00 (at 20 °C), 100 mM KCl. A 30-s time delay accompanied by constant shaking preceded the measurements. This allowed the assay mixture to reach both a uniform medium temperature and a medium homogeneity. Enzymatic reactions were always read in triplicate.

LDH activity was analyzed while taking into account its substrate inhibition kinetic peculiarity (Fig. 1). When the cofactor (β-NADH) is at saturating levels the LDH kinetics is described by the equation [2,22,23]

$$\upsilon = \frac{V'_{\max}[\mathrm{S}]}{K'^{\mathrm{PYR}}_{\mathrm{m}} + [\mathrm{S}] + \frac{[\mathrm{S}]^2}{K^{\mathrm{PYR}}_{\mathrm{si}}}}, \tag{2}$$

Table 1
Dilution factors applied to 1% tissue homogenates used to measure LDH kinetic parameters at different temperatures

Temperature (°C)	Muscle
4	50
8	80
12	110
16.5	160
21	250
25.5	375
30	500

where $V'_{\max}$ is the maximal (limiting) rate of pyruvate reduction (U mg protein^{-1}), $K'^{\mathrm{PYR}}_{\mathrm{m}}$ is the Michaelis–Menten constant for pyruvate (mM), and $K^{\mathrm{PYR}}_{\mathrm{si}}$ is the substrate inhibition constant for pyruvate (mM) [2]. $V'_{\max}$ and $K'^{\mathrm{PYR}}_{\mathrm{m}}$ satisfy the usual conditions of the Michaelis–Menten parameters in the simple two-step model; however, they are written with primes because they are not exactly Michaelis–Menten parameters. The effect of the term $[\mathrm{S}]^2$ is to make the rate approach zero rather than $V'_{\max}$ when [S] is large, and $K'^{\mathrm{PYR}}_{\mathrm{m}}$ is not equal to the value of [S] when $\upsilon = V'_{\max}/2$ [2].

Nonlinear regression analysis was used for the calculation of all kinetic parameters and for curve fitting [24]. $V'_{\max}$ from Eq. (2) always exceeds the actual reaction maximum rate ($\upsilon_{\max}$; open circle in Fig. 1), therefore, to calculate $\upsilon_{\max}$ the υ has to be differentiated with respect to [S] and then a value of [S] at which the slope of the curve reaches zero ($[\mathrm{S}]_{\max}$) can be identified as [22] follows:

$$[\mathrm{S}]_{\max} = \sqrt{K'^{\mathrm{PYR}}_{\mathrm{m}} K^{\mathrm{PYR}}_{\mathrm{si}}}. \tag{3}$$

Substituting this value into Eq. (2) yields $\upsilon_{\max}$:

$$\upsilon_{\max} = \frac{V'_{\max}}{1 + 2\sqrt{\frac{K'^{\mathrm{PYR}}_{\mathrm{m}}}{K^{\mathrm{PYR}}_{\mathrm{si}}}}}. \tag{4}$$

The specific LDH activity was expressed as µmol of NADH oxidized per minute per mg of total protein (U mg protein^{-1}) using 6.22×10^3 as an extinction coefficient of NADH [19].

Temperature-controlled microplate (T-microplate) for a 96-well microplate reader

A temperature-controlled microplate was produced from a redesigned conventional microplate (Greiner bio-one; 96-well, polystyrene, F-bottom, with nonbinding protein capacity) with dimensions (L × W × H, mm) $127.76 \times 85.47 \times 14.22$ [25]. The distinguishing feature of this particular microplate is that it has empty space around the wells that is accessible from the bottom side of the microplate. The bottom side of the microplate was covered with a transparent and spectrophotometric grade glass plate (1 mm thickness) and the internal cavity (52 ml) filled with heat-exchanging fluid (Fig. 2B). Additional inlets and outlets were built into the wall of the T-microplate (Fig. 2A). The T-microplate was connected to an external thermostat (PolyScience 9105) by means of insulated flexible tubes (Fig. 2C). The external thermostat was filled with transparent and spectrophotometric-grade heat-exchanging fluid (50% ethylene glycol), which was pumped through the deadspace of the T-microplate. All air bubbles were thoroughly expelled from the T-microplate. The mass of the completely loaded T-microplate (including mass of the heat-carrier and 300 µl well^{-1} of samples) was 165.5 g.

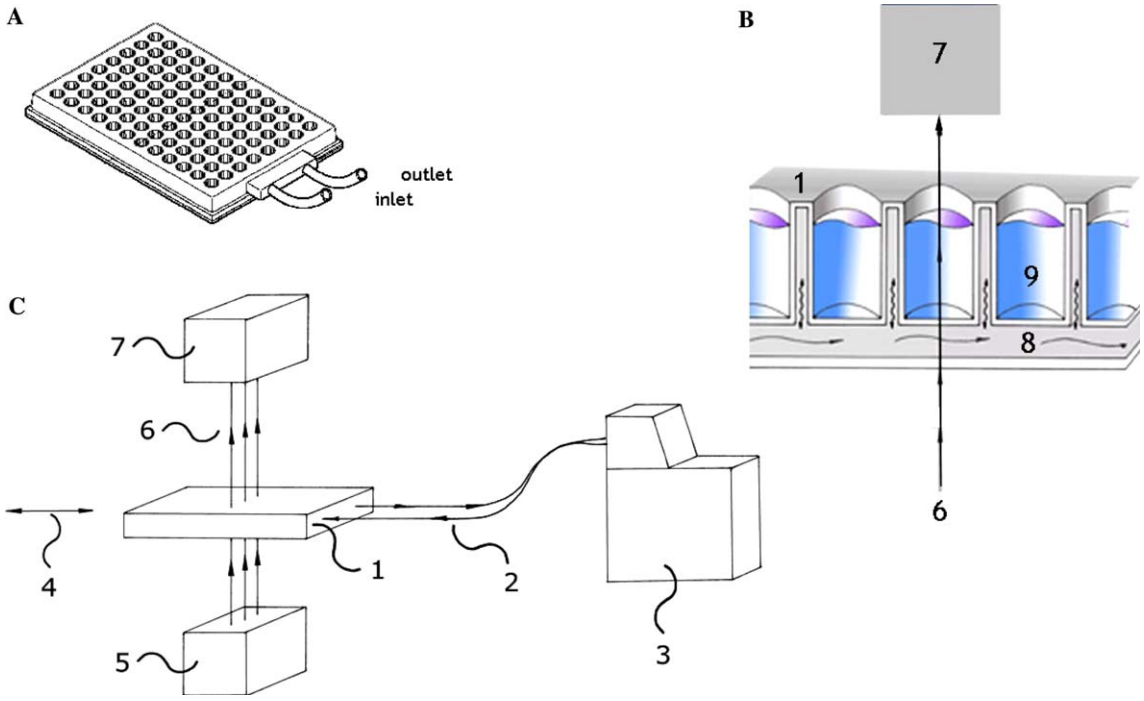

Fig. 2. (A) Three-dimensional view of the T-microplate; (B) three-dimensional cross section of the T-microplate in the course of operation; (C) main operational principal of the T-microplate. 1, T-microplate; 2, insulated flexible tubes; 3, external thermostat; 4, movement directions of T-microplate in the measuring chamber of a microplate reader; 5, schematic presentation of a light source of a microplate reader; 6, light beams; 7, schematic presentation of a photodetector of a microplate reader; 8, internal cavity of the T-microplate filled with heat carrying fluid and schematic presentation of its flow; 9, a well of the T-microplate filled with a liquid sample.

The T-microplate has been designed for applications in the wavelength range between 300 and 900 nm. These limits exist because of the optical properties of the polystyrene and the heat-carrier. Both significantly absorb the light at <280 nm but do not significantly interfere with analyzes at >340 nm. The average light absorption of the heat-carrier between 300 and 900 nm is $0.0122 \pm 4 \times 10^{-6}$ O.U. at 4 °C, which is only 0.6% of the total 2-O.U. optical range typical for any microplate reader. The level of optical absorption of the heat-carrier depends on temperature, but this dependence is only quantitative between 4 and 60 °C and does not come higher than 1.5% (at 60 °C) of the total 2-O.U. optical range. Therefore the zero level can be easily corrected.

The T-microplate was fitted into a Bio-Rad UV3550 microplate reader. However, the lid of the measuring chamber had to be removed. Therefore, measurements were carried out in a dark room. The external connecting flexible tubes allowed free movements of the T-microplate in the measuring chamber of the microplate reader during both measurement and shaking periods (Fig. 2C).

For the testing of the T-microplate thermal performance the T-microplate loaded with deionized water samples (300 μl) was mounted in a microplate carrier (''sledge'') and the samples temperature was measured by a thermocouple thermometer (DOSTMANN P500 with probe Pt100; accuracy ±0.1 °C) immersed into an aquatic sample.

The T-microplate is not disposable. We designed a simple 96-tip dispenser suitable for applying approximately 300 μl simultaneously in 96 wells and a 96-tip vacuum sucker for rapid cleaning. The T-microplate was rinsed three times with 50 mM Hepes, pH 7.00 (at 20 °C), and 100 mM KCl after each use. Also the microplate with the lowest protein affinity has been chosen for the construction of the T-microplate. This development has been patented [6].

Temperature-dependent kinetic parameters and the thermodynamics of LDH

The kinetic properties of LDH (V'_{max}, K'^{PYR}_m, K^{PYR}_{si}) were determined at seven assay temperatures (4, 8, 12, 16.5, 21, 25.5, and 30 °C) using the T-microplate (Fig. 3). The dilution factor of the homogenate was changed according to the assay temperature (Table 1) to keep assay conditions within the limits of linearity for the initial rate of the LDH reaction.

The temperature dependence of V'_{max} (Eq. (2)) and υ_{max} (Eq. (4)) was used to calculate the apparent Arrhenius activation energy (E_A; J mol^{-1}). Values of E_A were calculated from Arrhenius plots ($10^3/T$ K versus $\ln(\upsilon_{max})$ or $\ln(V'_{max})$) by use of the classic method via

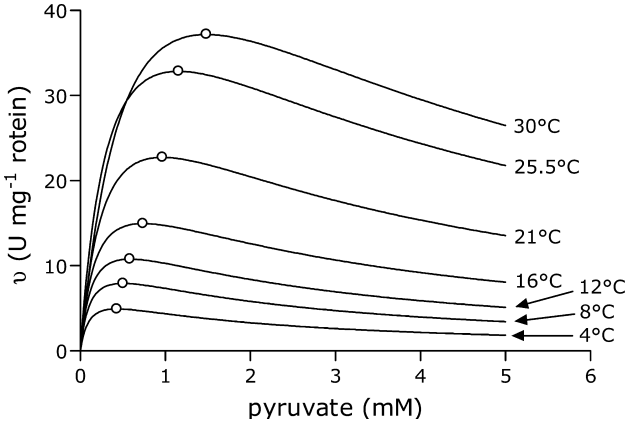

Fig. 3. υ_{max}s (open circles, for reference see Eq. (4)) were used to calculate the Arrhenius activation energy (E_A) of LDH with regard to substrate inhibition. An Arrhenius plot ($1/T$ versus $\ln(\upsilon_{max})$) was used to calculate E_A, which is $54.89 \pm 0.23\,kJ\,mol^{-1}$ ($R^2 = 0.950$, $n = 210$) in this particular example, where n is the total number of enzymatic reactions, which were read at 10 pyruvate concentrations and at seven assay temperatures in triplicate to evaluate E_A for each individual fish.

regression slopes ($E_A = -\text{slope} \times R$, where R is the universal gas constant [$8.31434\,J\,mol^{-1}\,K^{-1}$]) (Fig. 8). Correspondingly, E_As were denoted as $E_A[V'_{max}]$ (based on the temperature dependence of V'_{max}) and $E_A[\upsilon_{max}]$ (based on the temperature dependence of υ_{max}).

The activation enthalpy change ($\Delta H^{\ddagger}$; $J\,mol^{-1}$) for LDH at the respective acclimation temperatures was calculated according to the equation

$$\Delta H^{\ddagger} = E_A - RT, \tag{5}$$

where R is the universal gas constant ($8.31434\,J\,mol^{-1}\,K^{-1}$) and T is the acclimation temperature (K).

To calculate the activation entropy change ($\Delta S^{\ddagger}$; $J\,mol^{-1}\,K^{-1}$) for nonpurified enzyme preparations we used the "compensation plot" for purified LDH from different sources, as compiled from the literature [9,26–32] (Fig. 4).

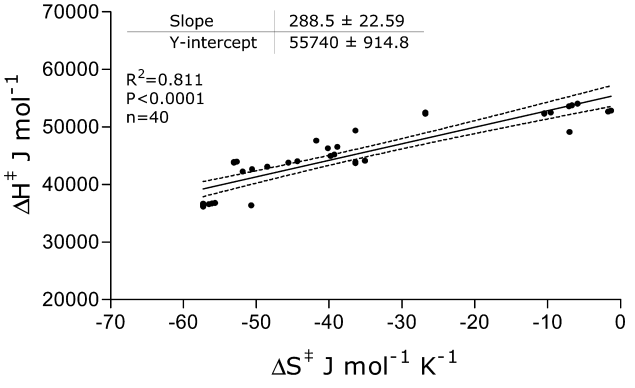

Fig. 4. Enthalpy–entropy "compensation plot" for pure preparations of the LDH as compiled from the literature (filled circles) [9,26–32]. The "compensation temperature" is 288.5 K (15.5 °C). The results of the linear regression are given as values ± SE. The dashed line is the 95% confidence interval for the regression equation.

The Gibbs free-energy change ($\Delta G^{\ddagger}$) of LDH in crude homogenate was computed for corresponding acclimation temperatures [31].

$$\Delta G^{\ddagger} = \Delta H^{\ddagger} - T\Delta S^{\ddagger}. \tag{6}$$

Since apparent Arrhenius activation energies can be calculated only for the temperature dependence of maximal reaction rates, we used the Q_{10} factor to quantify the temperature dependence of K_m^{PYR} and K_{si}^{PYR}. The Q_{10} factor has been calculated according to [32]:

$$Q_{10} = \left(\frac{\upsilon(T + \Delta T)}{\upsilon(T)}\right)^{\frac{10}{\Delta T}}. \tag{7}$$

Reagents

All reagents have been obtained from Sigma. A NanoOrange Protein Quantitation Kit (Molecular Probes) was used to determine the total protein concentration in diluted homogenates.

Statistics

Nonlinear regression analysis and curve fitting was performed with GraphPad Prism [33]. The temperature dependence of kinetic parameters was fitted to exponential equations with two parameters ($y = a \times \exp(bx)$). The temperature dependence of kinetic parameters was compared by use of F tests for a comparison of entire curves obtained by nonlinear regression [34]. When a significant difference between entire curves was found, we used an unpaired t test to determine which component of the regression equation had changed significantly [34]. Two-phase linear regression analysis was carried out according to Motulsky [33].

Results

T-microplate

The T-microplate is able to accurately control assay temperatures between the freezing point of the liquid sample and values up to 60 °C. The temperature set was linear relative to ambient temperature between 0 and 60 °C (Fig. 5). Within this temperature range the accuracy of the temperature control was ±0.1 °C, depending on the accuracy of the external thermostat. Temperature homogeneity (i.e., the temperature difference across the microplate) was ±0.3 °C at the lowest temperature tested (4 °C). The upper temperature limit of the T-microplate (60 °C) is set by the thermal properties of the polystyrene; the lower temperature limit of the T-microplate is set by the freezing point of the liquid sample.

However, the temperature in the T-microplate does not exactly correspond to the temperature of the

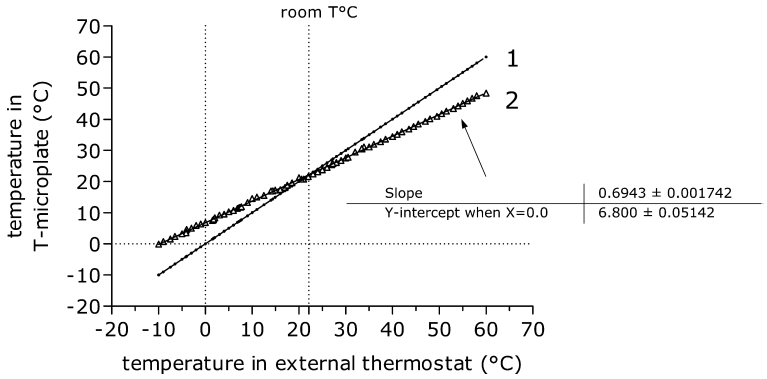

Fig. 5. Linear relationship between temperatures in the external thermostat (1) and the T-microplate (2). The results of the linear regression for line 2 are given as slope ± SE.

external thermostat, because of unavoidable heat loss. Therefore, to reach the desired temperature in the T-microplate a linear equation was used (Fig. 5). This equation depends on the particular constructional features of the device and on room temperature. Blowing of warm air (30 °C) through the measuring chamber makes temperature control independent of room temperature fluctuations and prevents water condensation on the T-microplate at low temperature (<6 °C).

Due to the high specific heat of the heat carrier ($0.82\,\mathrm{cal\,g^{-1}\,K^{-1}}$ at 25 °C) the time required to stabilize the final temperature in the preconditioned sample solution is relatively short (about 30 s). That is why we used a 30-s time lag before recording the reaction kinetics.

After each use the T-microplate was rinsed three times with Hepes buffer, and we did not detect any residual LDH activity thereafter.

Temperature dependence of kinetic parameters

Twenty one cod were acclimated to 4 °C for a long time (408 days) and then analyzed for temperature dependence of the kinetic parameters of LDH in crude homogenates of muscle tissue; 4204 enzymatic reactions in total were read at 10 pyruvate concentrations and seven assay temperatures in triplicate to obtain this information ($21 \times 10 \times 7 \times 3$; Table 2, Figs. 6 and 7). However, the total number of "useful" data points that was used for calculation of the kinetic parameters was 3969 ($21 \times 9 \times 7 \times 3$) of the total 4204, since $[S] = 0$ is not participating in the calculation. T-microplate and microplate reader Bio-Rad UV 3550 were used for the analysis. Ten days in total were spent to analyze this particular group of fish. An example of the set of kinetic parameters measured during the research is presented in Table 2.

LDH from cod showed very clear substrate inhibition kinetics (Fig. 1), as usually seen for LDH.

All studied kinetic parameters (V'_{max}, K'^{PYR}_m, and K^{PYR}_{si}) displayed very pronounced exponential dependence on assay temperature (Figs. 6 and 7). We used nonlinear regression analyzes with a two-parameter exponential equation ($y = a \times \exp(bx)$) to fit the data. The analyses of kinetic parameters were performed for temperatures between 4 and 30 °C. Elevated temperatures (>30 °C) resulted in an acute decrease of enzyme activity (data not shown), which may indicate thermal inactivation of the enzyme. However, even an assay temperature of 30 °C already results in a significant deviation of activities from the general trend. This conclusion originated from the observation that the values of R^2 for regression curves became considerably higher once values at 30 °C were omitted. At the same time, the absolute sum of square (ASS) and the standard deviation of the residuals (Sy.x) became considerably lower. Such omission increased R^2 to 0.999. Additionally, the

Table 2
Kinetic parameters of LDH in crude white muscle homogenates of Atlantic cod (*Gadus morhua*) exemplified for measurements at assay temperature equal to acclimation temperature (4 °C)

Parameter	Value ± SE	Units
Acclimation temperature	4	°C
Assay temperature	4	°C
V_{max}	7.51 ± 0.86	U mg prot^{-1}
K'^{PYR}_m	0.113 ± 0.014	mM
Q_{10} for K^{PYR}_m	1.94 ± 0.16	between 4 and 25 °C
K^{PYR}_{si}	1.64 ± 0.20	mM
Q_{10} for K^{PYR}_{si}	1.56 ± 0.12	between 4 and 25 °C
$[S]_{max}$	0.38 ± 0.02	mM
υ_{max}	4.70 ± 0.50	U mg prot^{-1}
[Protein]	49.87 ± 3.42	mg gww^{-1}
n_1	30	
n_2	21	
n_{total}	630	

V'_{max}, maximal rate of reaction (Eq. (2)); K'^{PYR}_m, constant of Michaelis–Menten for pyruvate (Eq. (2)); K^{PYR}_{si}, constant of substrate inhibition (Eq. (2)); Q_{10}, Q_{10} factor (Eq. (7)); $[S]_{max}$, substrate concentration at which the reaction rate has reached its maximum (Eq. (3)); υ_{max}, actual maximal rate of reaction (Eq. (4)); [Protein], concentration of total protein in the tissue; gww, gram wet weight (g); n_1, number of enzymatic reactions, read at 10 pyruvate concentrations in triplicate for every individual; n_2, total number of analyzed fish; n_{total}, number of enzymatic reactions, read to calculate kinetic parameters. See Fig. 1 for illustration.

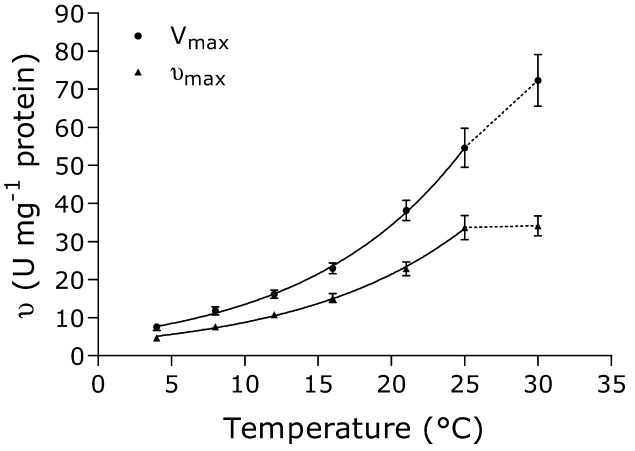

Fig. 6. Temperature dependence of V'_{max} (circles) and υ_{max} (triangles) of the LDH suite in crude homogenates of white muscle tissue from Atlantic cod *Gadus morhua* acclimated to 4 °C. The values of V'_{max} and υ_{max} at T 30 °C deviate significantly from the fitting curves (indicated by dashed lines); therefore, they were omitted from further calculations. This step increased the R^2 of the fit to $R^2 = 0.9998$ and $R^2 = 0.9996$, respectively. Values are means ± SE ($n = 21$, number of analyzed fish).

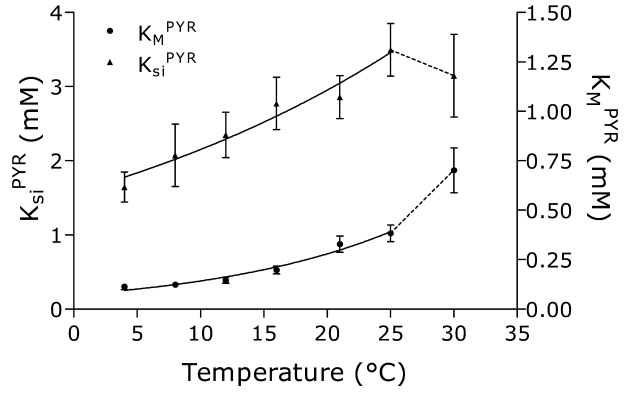

Fig. 7. Temperature dependence of substrate inhibition (K_{si}^{PYR}) and Michaelis–Menten constants ($K_m'^{PYR}$) for pyruvate determined for the LDH suite obtained from crude muscle homogenates of cod *Gadus morhua* acclimated to 4 °C. The values of K_{si}^{PYR} and $K_m'^{PYR}$ at 30 °C deviate significantly from the fitting curves (indicated by dashed lines); therefore, they were omitted from the calculations and this step has increased R^2 of the fit to $R^2 = 0.9977$ and $R^2 = 0.9948$, respectively. Values are means ± SE ($n = 21$, number of analyzed fish).

high values of R^2 indicate that the chosen exponential function adequately fits the data. Consequently, the rate values at 30 °C were omitted from further calculations (Fig. 6). Application of the F test to entire curves [33] revealed a significant difference between them ($P < 0.001$). Further use of the unpaired t test revealed a significant difference ($p < 0.01$) between quantitative components (a) of the regression equation, indicating clearly significant differences between these curves.

Similar observations apply to the temperature dependence of $K_m'^{PYR}$ and K_{si}^{PYR} (Fig. 7). Inclusion of values from assays at 30 °C significantly worsens all parameters of the fit (R^2, ASS, and Sy.x). The omission of these values increased R^2 to 0.995–0.997. Therefore, constants obtained at 30 °C were not included in calculations of Q_{10} (Table 2).

Thermodynamic parameters

We used seven assay temperatures (4–30 °C) to measure the temperature dependence of kinetic parameters (V'_{max}, $K_m'^{PYR}$, K_{si}^{PYR}). Then the temperature dependence of this set of kinetic parameters was recalculated to the temperature dependence of υ_{max} (Eq. (4)).

In general, 210 enzymatic reactions at different assay temperatures were read to measure the temperature dependence of kinetic parameters in enzyme preparations from a single animal. We used 21 fish for these measurements, which resulted in 4204 enzymatic reactions of the total 4410 excluding those rate values that were not statistically satisfactory (see n_1 and n_2 in Table 3).

Analysis of Arrhenius plots (Fig. 8) for the temperature dependence of V'_{max} and υ_{max} revealed that there is a general difference between the two lines (F test, $p < 0.05$) and the consecutive unpaired t test demonstrated that the difference originated from a significant difference between quantitative components (a) ($p < 0.05$) of the linear regression equation ($y = a + bx$), but there was no difference between the slopes.

Use of the unpaired t test in a comparison of the two methods to calculate the thermodynamic properties of LDH (E_A, $\Delta H^{\ddagger}$, $\Delta S^{\ddagger}$, and $\Delta G^{\ddagger}$) via the temperature dependence of either V'_{max} or υ_{max} did not reveal differences between these methods ($p > 0.05$). This test also suggests that the difference between the two SDs is also nonsignificant. Moreover, the medians of the thermodynamic parameters obtained by the different methods are almost identical (Table 3).

High values of R^2 (Table 3 and an example in Fig. 8) implies that there was no break point in the Arrhenius plot between 4 and 25 °C. Consequently, there was no conformational change in the LDH molecule over the investigated temperature range.

Discussion

T-microplate

This technological improvement of temperature control in a 96-well microplate reader allowed analysis of the temperature dependence of kinetic parameters and the thermodynamic properties of enzymes from ectothermic animals within the temperature range that the animals normally experience under natural conditions (e.g., 0–30 °C). Such application of the microplate technique was not possible before, because of lack of the corresponding device.

Table 3
Thermodynamic parameters of LDH activity in crude muscle homogenates of Atlantic cod (*Gadus morhua*) calculated for the acclimation temperature

Parameter based on temperature dependence of	Value ± SE		Units	Difference
	V'_{max}	υ_{max}		
AT	4		°C	
E_A Average	65.14 ± 3.21	62.88 ± 2.45	kJ mol^{-1}	*ns*
Median	64.30	63.67	kJ mol^{-1}	
R^2 for Arrhenius plot	0.925 ± 0.020	0.958 ± 0.012		
$\Delta H^{\ddagger}$ Average	62.83 ± 3.21	60.57 ± 2.45	kJ mol^{-1}	*ns*
Median	61.99	61.36	kJ mol^{-1}	
$\Delta S^{\ddagger}$ Average	24.61 ± 11.13	16.77 ± 8.50	J mol^{-1} K^{-1}	*ns*
Median	21.69	19.50	J mol^{-1} K^{-1}	
$\Delta G^{\ddagger}$ Average	56.02 ± 0.13	55.93 ± 0.10	kJ mol^{-1}	*ns*
Median	55.98	55.96	kJ mol^{-1}	
n_1	21			
n_2	4204			

AT, acclimation temperature; E_A, apparent Arrhenius activation energy (kJ mol^{-1}); $\Delta H^{\ddagger}$, activation enthalpy change (kJ mol^{-1}); $\Delta S^{\ddagger}$, activation entropy change (kJ mol^{-1}); $\Delta G^{\ddagger}$, Gibbs free-energy change (kJ mol^{-1}); R^2, squared Pearson correlation coefficient for the slope of the Arrhenius plot; n_1, number of analyzed fish; n_2, total number of enzymatic reactions, read for n_1 fish at 10 pyruvate concentrations, at seven temperatures, and in triplicate to calculate mean E_A and SE; *ns*, the difference between compared parameters is not significant (unpaired *t* test; $p < 0.05$).

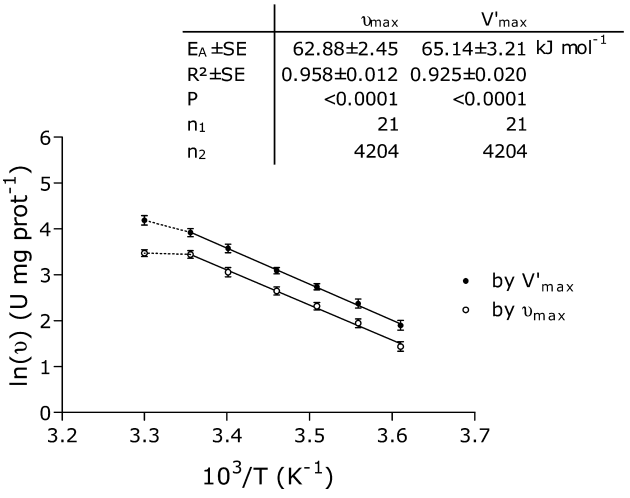

Fig. 8. Example of the Arrhenius plot based on the temperature dependence of V'_{max} and υ_{max} for the overall LDH suite from white muscle of cod *Gadus morhua* acclimated to 4 °C; υ_{max}, actual maximum level of the reaction rate (Eq. (4)); V'_{max}, theoretical maximum reaction rate (Eq. (2)); n_1, number of analyzed fish; n_2, total number of enzymatic reactions, read at 10 pyruvate concentrations and seven assay temperatures in triplicate to evaluate the temperature dependence of kinetic parameters. The values of V'_{max} and υ_{max} at 30 °C were omitted from the calculation because of the onset of thermal inactivation (Fig. 6) (see the dashed line).

The multiple-use T-microplate was equipped with a vacuum cleaner designed to ensure proper cleaning after each use. Also the microplate with the nonbinding protein capacity has been chosen for the construction of the T-microplate. Since we worked on diluted homogenates (the dilution factor of tissue samples ranged up to 5×10^4; Table 1) and adequately rinsed the T-microplate after each use, we have assumed that protein binding to the microplate surface should be negligible. This assumption has been collaborated by the lack of residual LDH activities in the T-microplate after the rinsing procedure.

Temperature homogeneity across the T-microplate was ±0.3 °C at 4 °C. The closer that the temperature of the T-microplate approached to room temperature the higher was the temperature homogeneity achieved. The temperature homogeneity across the T-microplate that was reached under extreme conditions (4 °C) is higher than that obtained in most commercial microplate readers with temperature control under mild conditions. Another advantage of the T-microplate is that the high specific heat of the heat-carrier allows fast cooling/warming of the samples within less than 30 s as it is suitable for rapid kinetic analyses.

Thus, using the T-microplate we were able to analyze 21 fish within a relatively short time (10 days). For each individual fish the temperature dependence of enzyme kinetics was read at a statistically satisfying level (at 10 pyruvate concentrations under seven temperatures in triplicate). This approach of temperature control in the microplate allowed Zhakartsev et al. [35] to study the temperature dependence of LDH kinetic and thermodynamic parameters for an even larger number of fish ($n = 36$) acclimated to different temperatures with the same high-throughput system.

Kinetics

LDH in crude homogenates of cod *G. morhua* always comprises the full set of allo- and isoenzymes, which includes products of at least three *Ldh* loci (*A*, *B*, and *C*)

[13]. Protein polymorphism at the locus *Ldh-B* due to two alleles *a* and *b* determines the *Ldh-B* phenotype of an animal as *a*/*a*, *a*/*b*, and *b*/*b* [13,36]. All allo- and isozymes are expressed simultaneously, but the final allo/isozyme pattern depends on the tissue and the *Ldh-B* phenotype. Functional consequences of the electrophoretic pattern of LDH in cod tissues are difficult to interpret. In the present study we use the term "overall LDH suite" (LDHs mixture) to stress that we worked on crude homogenates of cod muscle, where all these allo/isoenzymes were present. Accordingly, we have evaluated the resulting (net) kinetic parameters of the LDH mixture as it is operative in vivo.

To calculate K'^{PYR}_m, K^{PYR}_{si}, and V'_{max} values of LDH we used nonlinear regression analyzes, instead of classical linear transformations, because the linear transformation amplifies and distorts the scatter, and thus the linear regression does not yield the most accurate values of kinetic parameters [37], especially in the case of substrate inhibition.

In general, it is well documented that LDH from most ectothermic animals displays peculiar kinetic properties characterized by high levels of substrate inhibition [7–14]. This means that, at low substrate concentrations, the reaction follows normal Michaelis–Menten kinetics but, when substrate concentrations reach high level, the inhibition sets in. In this way the reaction rate never reaches its theoretical limiting level (V'_{max}) [2]. The substrate inhibition phenomenon in LDH is caused by the formation of an inactive covalent adduct between the pyruvate and the oxidized form of the cofactor, i.e., the formation of an abortive LDH–NAD^+–pyruvate complex [15,16]. In general, the mechanism of high substrate inhibition is analogous to that usually considered for uncompetitive inhibition [2,38].

Depending on assay temperature, all kinetic parameters (V'_{max}, υ_{max}, K'^{PYR}_m, K^{PYR}_{si}) followed an exponential curve with very high R^2 between 4 and 25 °C (0.994–0.999). Thorough statistical analysis revealed that at 30 °C all kinetic parameters significantly deviated from the exponential relationship, evidenced by considerable worsening of the fit (according to R^2, ASS, and Sy.x). These observations indicate that temperatures beyond 25–30 °C cause onset of thermal inactivation of muscle LDH from cod acclimated to 4 °C.

Two-phase linear regression analyzes of the temperature dependence of K'^{PYR}_m showed that at assay temperatures below 16 ± 1 °C the K'^{PYR}_m of the overall LDH suite is almost temperature independent at a slope of 0.0041 mM per degree. Such temperature increment of the constant gives only 3.5% of absolute value of the K'^{PYR}_m at 4 °C. Evidently, the affinity of LDH to pyruvate is not significantly affected by temperature variation within this range. This must have important consequences for the enzyme under physiological conditions (low substrate concentrations), in that the enzyme becomes insensitive to temperature fluctuations below 16 °C. It appears that the enzyme is well suited to tolerate rapid fluctuations of habitat temperatures on top of the general seasonal trend. This excludes the necessity to express different isozymes depending on the season [35].

The technique of temperature control in microplates developed in this study has been applied for the parallel study of acclimation effects of Atlantic cod to seasonal temperature variation [35] and it has demonstrated its efficiency. Despite earlier studies reporting kinetic differences between LDH allozymes [9] our parallel study [35] of crude tissue homogenates of cod *G. morhua* could not reveal kinetic differences (in V'_{max}, K'^{PYR}_m, K^{PYR}_{si}, protein concentration, and E_A) among *Ldh-B* phenotypes (overall LDH suites). Very likely, this is due to the relatively small fraction (14–19%) of LDH-B allozymes in the overall LDH suite, such that kinetic differences become invisible in the overall mixture.

Thermodynamics

The calculation of apparent Arrhenius activation energies (E_A) for enzymatic reactions is commonly based on the temperature dependence of rate measurements at saturating concentrations of a substrate (i.e., V_{max}s), when substrate availability will not be limiting for the reaction rate [1]. However, in the case of high-substrate inhibition kinetics of LDH, the calculated V'_{max} never coincides with the actual maximal rate of the reaction (υ_{max}), and they may have different thermal behavior. Accordingly, we calculated both the apparent E_A by use of the temperature dependence of V'_{max} and the actual E_A by use of the temperature dependence of υ_{max}. Both lines yielded similar slopes of Arrhenius plots that resulted in nondistinguishable E_A values. This fact indicates similar thermal behavior of V'_{max} and υ_{max} (Table 3). Consequently, it is not surprising that we found no difference in $\Delta G^{\ddagger}$ between calculation methods (Table 3). Absence of break points in the Arrhenius plot (confirmed by high R^2; Table 3) excludes conformational state transitions over the studied temperature range (4–25 °C). These results were obtained with a high level of precision for a large number of animals and we think that the use of the microplate technique has considerably increased the quality of the collected dataset.

General conclusions

High sample throughput by use of a 96-well microplate reader with enhanced temperature control allowed the collection of a large dataset at a high level of statistical reliability. The overall LDH suite in crude homogenates of muscle from Atlantic cod *G. morhua*

acclimated to 4 °C displayed $K_m'^{PYR}$ values insensitive to temperature below 16 °C; 25 °C is probably the temperature where unfolding of the molecules sets in and causes a decrease of enzyme activity (V'_{max} or υ_{max}).

The T-microplate has also been used in a parallel study of LDH adaptation in different tissues (muscle and liver) from Atlantic cod *G. morhua* (North Sea population) acclimated to 4 and 12 °C [35]; the T-microplate showed exceptional performance and demonstrated its efficiency. We observed that $K_m'^{PYR}$ did not change with acclimation, whereas K_{si}^{PYR} underwent significant lowering in the cold. At the same time, we did not find an expression of additional LDH isozymes or a change in the p*I* of any LDH allo/isozymes. We also observed that E_A for LDH increased with acclimation to the lower temperature (4 °C), but $\Delta G^{\ddagger}$ remained the same. One possible reason for the E_A increment is the introduction of an additional weak (noncovalent) bond into the LDH molecule [32]. As a result the molecule becomes more rigid, because the protein conformation is stabilized, and E_A increases in due course. This conformational change is potentially beneficial at low-temperature acclimation, because both aerobic and anaerobic metabolism compete for pyruvate. The modification in the LDH molecule will shift the use of pyruvate in favor of aerobic metabolism. As recently reviewed by Pörtner [39,40], capacity limitations of aerobic metabolism set the limits of thermal tolerance in ectothermic animals. The observed adaptation patterns in LDH are in line with this concept.

Acknowledgments

The work was supported by EU Project CLICOFI "Effects of climate induced temperature change on marine coastal fishes" (ENV4-CT97-0596). The authors thank Professor G. Nævdal and Dr. T. Johansen (University of Bergen, Norway) for extended collaboration in this research.

References

[1] I.H. Segel, Biochemical calculations: how to solve mathematical problems in general biochemistry, Wiley, New York, 1976.
[2] A. Cornish-Bowden, Fundamentals of enzyme kinetics, Portlend Press, London, 1995.
[3] R.R. Sokal, F.J. Rohlf, Biometry. The principles and practice of statistics in biological research, W.H. Freeman and Company, New York, 1995.
[4] S. Beck, UV/Vis microplate readers, Scientist 12 (1998) 18–20.
[5] Molecular Devices Corporation, SPECTRAmax GEMINI dual-scanning microplate spectrophotometer operator's manual, Molecular Devices Corporation, California, USA, 1999.
[6] M.V. Zakhartsev, R. Blust, Temperature-controlled device and method suitable for spectroscopic analysis. European Patent EP 1 266 691 A1. Belgium, 2002.
[7] J. Baldwin, W. Davison, M.E. Forster, Properties of the muscle and heart lactate dehydrogenases of the New Zealand hagfish, *Eptatretus cirrhatus*: functional and evolutionary implications, J. Exp. Zool. 250 (1989) 135–139.
[8] J. Narita, S. Horiuchi, Effect environmental temperature upon muscle lactate dehydrogenase in the crayfish, *Procambarus clarki* Girard, Comp. Biochem. Physiol. B 64 (1979) 249–253.
[9] A.R. Place, D.A. Powers, Kinetic characterization of the lactate dehydrogenase (LDH-B4) allozymes of *Fundulus heteroclitus*, J. Biol. Chem. 259 (1984) 1309–1318.
[10] V. Almedia-Val, M.L.B. Schwantes, A.L. Val, LDH isozymes in amazon fish—2. Temperature and pH effects on LDH kinetic properties from *Mylossoma duriventris* and *Colossoma macropomum* (Serrasalmidae), Comp. Biochem. Physiol. 98B (1991) 79–86.
[11] C.J. French, P.W. Hochachka, Lactate dehydrogenase isoenzymes from heart and white muscle of water-breathing and air-breathing fish from the Amazon, Can. J. Zool. 56 (1978) 769–773.
[12] H. Tsukuda, H. Yamawaki, Lactate dehydrogenase of goldfish red and white muscle in relation to thermal acclimation, Comp. Biochem. Physiol. B 67 (1980) 289–295.
[13] M.S. Zietara, E.F. Skorkowski, Purification and properties of the heart type lactate dehydrogenase of the cod (*G. morhua*) from the Baltic sae: Comparison with LDH-A4 and LDH-C4, Comp. Biochem. Physiol. B 105 (1993) 349–356.
[14] M.S. Zietara, J. Gronczewska, K. Stachowiak, E.F. Skorkowski, Lactate dehydrogenase in abdominal muscle of crayfish *Orconectes limosus* and shrimp (*Crangon crangon Decapoda: Crustacea*): properties and evolutionary relationship, Comp. Biochem. Physiol. B 114 (1996) 395–401.
[15] C.M. Eszes, R.B. Sessions, A.R. Clarke, K.M. Moreton, J.J. Holbrook, Removal of substrate inhibition in a lactate dehydrogenase from human muscle by a single residue change, FEBS Lett. 399 (1996) 193–197.
[16] C.O. Hewitt, C.M. Eszes, R.B. Sessions, K.M. Moreton, T.R. Dafforn, J. Takei, C.E. Dempsey, A.R. Clarke, J.J. Holbrook, A general method for relieving substrate inhibition in lactate dehydrogenases, Protein Eng. 12 (1999) 491–496.
[17] L.G. Ross, B. Ross, Anaesthetic and Sedative Techniques for Aquatic Animals, Blackwell Science, Oxford, 1999.
[18] T.H. Yang, G.N. Somero, Effects of feeding and food deprivation on oxygen consumption, muscle protein concentration and activities of energy metabolism enzymes in muscle and brain of shallow-living (*Scorpaena guttata*) and deep-living (*Sebastolobus alascanus*) scorpaenid fishes, J. Exp. Biol. 181 (1993) 213–232.
[19] R.M.C. Dawson, D.C. Elliott, W.H. Elliott, K.M. Jone, Data for Biochemical Research, Oxford University Press, Oxford, 1986.
[20] P.H. Yancey, G.N. Somero, Temperature dependence of intracellular pH: Its role in the conservation of pyruvate apparent K_m values of vertebrate lactate dehydrogenases, J. Comp. Physiol. B 125 (1978) 129–134.
[21] P.L.M. Van Dijk, C. Tesch, I. Hardewig, H.O. Pörtner, Physiological disturbances at critically high temperatures: a comparison between stenothermal antarctic and eurythermal temperate eelpouts (*Zoarcidae*), J. Exp. Biol. 202 (1999) 3611–3621.
[22] A. Cornish-Bowden, Basic Mathematics for Biochemists, Oxford University Press, Oxford, 1999.
[23] R. Eisenthal, M.J. Danson, Enzyme Assays: A Practical Approach, Oxford University Press, Oxford, UK, 2002.
[24] H. Motulsky, GraphPad Prism V 3.02, GraphPad Software, San-Diego, 2002.
[25] Society for Biomolecular Screening. Footprint dimentions for microplate. 1–8. 2003. Society for Biomolecular Screening.
[26] P.S. Low, G.N. Somero, Temperature adaptation of enzymes: a proposed molecular basis for the different catalytic efficicencies of enzymes from ectotherms and endotherms, Comp. Biochem. Physiol. B 49 (1974) 307–312.

[27] J. Baldwin, Selection for catalitic efficiency of lactate dehydrogenase M4. Correlation with body temperature and levels of anaerobic glycolysis, Comp. Biochem. Physiol. B 52 (1975) 33–37.
[28] V.Yu. Uvarov, A.I. Archakov, Compensational dependence of activation parameters of membrane enzymes, Biomed. Sci. 1 (1990) 617–621.
[29] G.N. Somero, P.S. Low, Temperature: a shaping force in protein evolution, Biochem. Soc. Symp. 41 (1976) 33–42.
[30] P.S. Low, J.L. Bada, G.N. Somero, Temperature adaptation of enzymes: role of the free energy, the enthalpy, and entropy of activation, Proc. Natl. Acad. Sci. USA 70 (1973) 430–432.
[31] C.L. Prosser, Adaptation Biology: Molecules to Organisms, Wiley, New York, 1986.
[32] P.W. Hochachka, G.N. Somero, Biochemical Adaptation, Princeton University Press, New Jersey, 1984.
[33] H. Motulsky, Analyzing Data with GraphPad Prism, GraphPad Software, San Diego, CA, 1999.
[34] H. Motulsky, The GraphPad Guide to Comparing Dose–response or Kinetic Curves, GraphPad Software, San-Diego, CA, 1998.
[35] M.V. Zakhartsev, T. Johansen, H.O. Pörtner, R. Blust, Effects of temperature acclimation on lactate dehydrogenase of cod (*G. morhua*): genetic, kinetic and thermodynamic aspects, J. Exp. Biol. 207 (2004) 95–112.
[36] W.S. Grant, G. Stahl, Description of electrophoretic loci in Atlantic cod, *G. morhua*, and comparison with Pacific cod, *Gadus macrocephalus*, Hereditas 108 (1988) 27–36.
[37] H. Motulsky, The GraphPad Guide to Nonlinear Regression, GraphPad Sowtware, San-Diego, CA, 1996.
[38] T. Palmer, Understanding Enzymes, Ellis Horwood, New York, 1991.
[39] H.O. Pörtner, Climate variations and the physiological basis of temperature dependent biogeography: systemic to molecular hierarchy of thermal tolerance in animals, Comp. Biochem. Physiol. A 132 (2002) 739–761.
[40] H.O. Pörtner, Physiological basis of temperature-dependent biogeography: trade-offs in muscle design and performance in polar ectotherms, J. Exp. Biol. 205 (2002) 2217–2230.